Hindawi
International Journal of Aerospace Engineering
Volume 2022, Article ID 7976691, 10 pages
https://doi.org/10.1155/2022/7976691

Research Article

Web Optimization of Compression Ignition Aviation Engine Crankshaft

Serkan Galata[1,2] **Yiğit Okur,**[1] **Ülkü Uzan,**[1] **Emre Ünlü,**[1] **Kudret Muhziroğlu,**[1] **Övün Işın**[2] **Mehmet Oğuz Turgut,**[1] **and Emin Tuzlu**[1]

[1]*TUSAŞ Engine Industries Inc., R&D Center, Piston Engines Department, Eskisehir, Turkey*
[2]*Yildiz Technical University, Mechanical Engineering Department, Internal Combustion Engines Laboratory, Istanbul, Turkey*

Correspondence should be addressed to Serkan Galata; serkan.galata@gmail.com

Received 16 October 2021; Revised 8 July 2022; Accepted 1 September 2022; Published 16 September 2022

Academic Editor: M Sekar

The focus of this study was the weight reduction of crankshaft web regions of an inline 4 cylinder, 250 HP compression ignition engine with a combustion chamber volume of 2499 cm^3 intended for use in aircraft. Iteration #0 model was generated by manual reduction of a reference model. According to the results of the analyses, the stresses were compared. Since the increase in stress values of weight reduced model over the reference model exceeded the targeted upper limit of 15.0%, three geometric parameters have been defined, and seven candidate design models have been created by using one, two, or all of the three parameters. In order to maximize the weight reduction by achieving the target stress limit, the lightest design model was obtained in the 10^{th} iteration. For the last three iterations, new parametric values were determined by utilizing the calculated effects of the geometric parameters on stress and weight.

1. Introduction

The combustion phenomenon occurs in internal combustion engines when air is transported to the combustion chamber and fuel enters, resulting in a chemical interaction. Fuel, either liquid or gas, contains molecules such as carbon, hydrogen, sulfur, and oxygen in varying amounts and bond types [1]. Combustion is started with an external factor such as a spark plug in an Otto engine; is started by injecting fuel into compressed air with increasing pressure and temperature in a Diesel engine. Chemical bonds in the hydrocarbon fuel are broken and energy is obtained as a result of combustion [2]. The piston moves downwards in a straight line due to the force imposed on its body. The connecting rod transfers this force to the crankshaft, resulting in rotational motion [3]. This movement is conveyed to the wheels of automobiles and to the propeller in aviation via the drivetrain.

The design of a crankshaft from scratch, or the process of modifying an engine to make it more powerful, is a significant task for design engineers [4, 5]. Crankshafts are subjected to a high number of cyclic stresses during their service life, which can lead to fatigue issues [6, 7]. As a result of the tremendous loads, they are subjected to, the crankshaft should have a strong and lasting structure while still being light due to inertia and centrifugal forces. Particularly in order to achieve high power density, today's engines must be designed to be lighter and more compact [8]. In the automotive sector, the tightening of emission values by international authorities has encouraged companies to build more environmentally friendly engines by enhancing fuel efficiency [9]. Today, in addition to gasoline and Diesel fuel which can be defined as standard fuels; alcohols such as methanol and ethanol; petroleum products such as liquefied petroleum gas; natural gas products such as compressed natural gas, adsorbed natural gas, liquefied natural gas can be used as alternative fuel for emission control and reduction of combustion-end temperatures. The use of chlorella microalgae biodiesel blends with carbon nanotubes and alumina improving sound and vibration levels of the engine besides emission especially PM [10, 11]. When accelerating the vehicle, reducing the weight of the rotating elements necessitates a lower power requirement [12]. Weight is one of the most essential design outputs, particularly in engine parts utilized in the aviation industry, because it directly impacts critical parameters such as take-off power, take-off weight, and airtime. Considering the contradicting requirements stated, the significance of the optimization process in crankshaft design is obvious.

The optimization applied to the web regions for weight reduction in a crankshaft designed for an inline 4 cylinder compression ignition engine planned to be used in aircraft was carried out in this study with the assistance of a computer-generated three-dimensional model of the part and finite element software.

2. Crankshaft Weight Reduction

The main purpose of internal combustion engine design is to attain low weight and cost values while maintaining good performance and durability. It is obvious that fuel consumption and emission values in automobiles are reduced as engine weight is reduced. As a result, more cost-effective and eco-friendly products can be produced. In several types of aviation engines, the ballast weight added to the aircraft's nose or tail decreases as engine weight lowers. Instead of this gain, additional fuel is added to extend flight time, or as an additional payload. For these reasons, along with strength, lightness is regarded as the most critical design criterion in aviation parts.

The crankshaft attracts attention in weight-reduction programs since it accounts for approximately 10% of total engine weight. Since the crankshaft is not a fixed part, care must be taken while choosing which area of the part to focus on for weight reduction. Removing material from different regions of the crankshaft may have distinct effects on the mass balancing ratio, deviation moment, or natural frequency of the crankshaft [13].

Crankshaft weight reduction strategies are basically classified as follows:

(i) Density shift

(ii) Reduction of combustion pressure

(iii) Variation in length and diameter of main bearing and crank pin

(iv) Geometry optimization

2.1. Density Shift. It has been observed that using aluminum in main engine components such as the cylinder block and cylinder head has resulted in significant weight savings. When this modification is made to the crankshaft, the volume values required to balance the forces; cause a weight increase, as do the package sizes. Tungsten plugs with a high density can be utilized in these instances [14]. However, because the applicability of this procedure is ineffective, the focus has been shifted to alternate manufacturing approaches. The cast-iron crankshaft is 10% lighter than the forged steel due to material and density differences. The fact that the casting process permits items to be manufactured in a hollow structure without machining presents the possibility of weight gain. Aside from the weight disadvantage of forged steel parts, expenses of producing and processing are significant, whereas cast iron crankshafts are inexpensive in large quantities [15]. Regardless, the forging method is commonly utilized in crankshafts. Micro-alloyed steel constructions attain high yield and tensile strength values, with improvements of 30-50% possibility [16]. The steel's high elasticity modulus improves NVH values and offers a high level of comfort to the vehicle user [12]. In high-performance engines, forged parts give excellent fatigue resistance [17, 18]. Because the probability of a porous structure in the casting method is great, and there is a risk of creating a notch effect, the forging method comes into prominence.

2.2. Reduction of Combustion Pressure. The power that produced in the combustion chamber impacts the piston crown and provides linear piston movement in internal combustion engines. The connecting rod transmits the movement to the crankshaft. During this force and motion transmission, the load; flows from the piston and connecting rod to the crankshaft and; the pin and main bearing regions of the crankshaft carry the combustion load. The diameters and widths of these bearings can be reduced, since the force to be transferred by reducing the combustion pressure will also decrease. Thus, the crankshaft becomes smaller and its weight is reduced. Moreover, counterweights on the crankshaft are employed to offset the inertia force generated during the piston's movement. The weight of the counterweights can be lowered by reducing the maximum gas pressure value in the combustion chamber [19]. Since the weight reduction with the related method is realized by compromising the power characteristics of the engine, the application of the method is not highly prioritized.

2.3. Variation in Length and Diameter of Journals. Mechanical losses in the power transmission system are created by pistons, connecting rods, crankshaft main bearings, and crank pins. Methods of reduction the diameter and width of the crankshaft's main bearings and pins are used to lessen these losses [20]. This method, which is used to reduce mechanical losses, also results in a significant improvement in crankshaft weight. However, as the surface pressure value operating on the crank pins increases, the strength limit of the connecting rod bearings becomes the limiting parameter in this reduction process. In addition, since reducing the width of the crankshaft will result in the cylinder block and reducing the crank pin diameter will result in changing the connecting rod geometries, it is more effective to use this method in the design phase of parts whose prototypes have not been produced yet.

2.4. Geometry Optimization. Focusing on local areas of the crankshaft's geometry provides the designer with numerous optimization options, including geometry optimization in counterweights, hollow shaft in main bearings and crank pins, and web shape optimization.

The drilling technique can be used on the main bearings and crank pins of the crankshaft. However, if the machining tool cannot reach the inner sections of the part and thus cause a limited amount of reduction, using this method may pose a risk. Hollow construction with cores that can

Table 1: Technical properties of engine and crankshaft.

Property	Unit	Value
Bore × Stroke	mm × mm	92 × 94
Stroke volume	cm^3	622
Number of cylinder	Quantity	4
Combustion chamber volume	cm^3	2499
Engine power	HP	250 @3500 rpm
Engine power	kW	186 @3500 rpm
Number of counter weight	Quantity	8
Diameter of main bearing journal	mm	65.00
Diameter of crank pin	mm	60.00

be used in the casting process can be created during the production phase [21]. According to the geometry designed for high speeds and high-power racing engines, the crankshaft can be machined in separate structures and combined with methods such as EBW [22].

The stress values on the counterweights and the webs are obtained as lower in crankshaft analysis than on the main bearings and crankpins [23]. As a result, crank web shape optimization can achieve the best web design by using structural optimization with the finite element method. Fatigue analysis should be performed in this method, especially in high-speed spark ignition engines, because crankshaft durability is critical as revolution increases [13].

3. Crankshaft Web Optimization

A crankshaft was designed within the scope of the study for an aircraft compression ignition engine with an inline 4 cylinder and combustion chamber volume of 2499 cm^3. The technical characteristics of the engine and crankshaft are presented in Table 1.

3.1. 3D Modeling. A 3D model of the part was created virtually by using Siemens NX 12.0.0.27 software, as shown in Figure 1. This model was used as a reference. Weight reduction was manually applied to the relevant part, determined in the box, and this model was defined as iteration #0, or the lightened model as shown in Figure 2. That is a weight reduction application with engineering foresight, however it remains above the 15% stress increase limit. For this reason, 3 design parameters were determined within the scope of the optimization study.

Geometry optimization was performed by focusing on the web regions of the lightened model and manually modifying them. The following operations were performed on the web regions of the lightened model in the study:

(i) Thickening of the web (from 0 to 1 mm)

(ii) An increase in the web angle (from 0 to 5°)

(iii) Extending the web radius (from 10 to 20 mm)

During the adaptation of an automotive engine for aviation, the torque and crankshaft speed is increased by 15.0% using the constant torque method [24]. However, in this study, it is accepted that the engine's speed and torque values will remain constant. The weight minimization is aimed while the stress increase does not exceed the limit of 15.0% according to the reference model analysis, instead of speed and torque. In the first step, the reference model was firstly compared to the lightened model (iteration #0), and then geometric optimization was performed on the lightened model using the diagram in Figure 3. The outputs, the weight reduction and the stress increase, obtained from the analyses of the iteration models were checked for the inconsistency, then the process was repeated by returning to the geometry optimization step as in the flow chart, if the consistency was not achieved. Finally, the ideal output was obtained by achieving the targeted stress values into account with the minimum weight.

Table 2 shows the first seven candidate designs created by focusing on and modifying the web regions of the crankshaft. The manually weight-reduced version of the reference model shown in Figure 1 was named iteration #0. The web area was thickened by 1 mm in iteration #1, which was developed over iteration #0. The web angle was increased by 5° in iteration #2. The web radius was increased from 10 to 20 mm in iteration #3. Iteration #4 combined the second and third iterations, iteration #5 combined the first and second iterations, and iteration #6 combined the first and third iterations. In iteration #7, the 1^{st}, 2^{nd}, and 3^{rd} iterations were combined.

3.2. Parameter Sensitivity Analysis. Following the first 7 manually and heuristically developed iterations, it was observed that the weight reduction potential of the crankshaft continued. The 2^3 full factorial DOE was developed in Minitab 2019.1.1 software to realize this potential. In this design of experiments study, there are 3 main parameters shown in Figure 4: Thickness, angle and radius of web regions. These 3 parameters are defined as 2 variables as thickness 0 and 1 mm; angle 0 and 5°; radius 10 and 20 mm. The stress increase and weight decrease of the additional 7 iterations, which were developed based on the iteration #0, and the correlation sensitivity between parameters were calculated. The factorial plot graph of the results obtained is demonstrated in Figure 4.

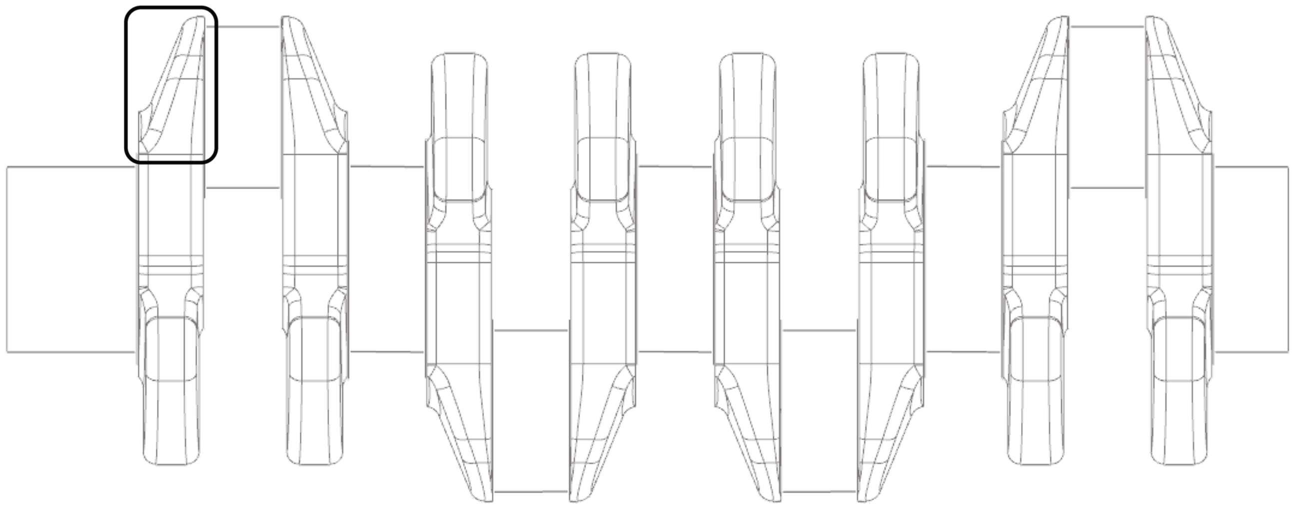

Figure 1: Reference crankshaft sketch.

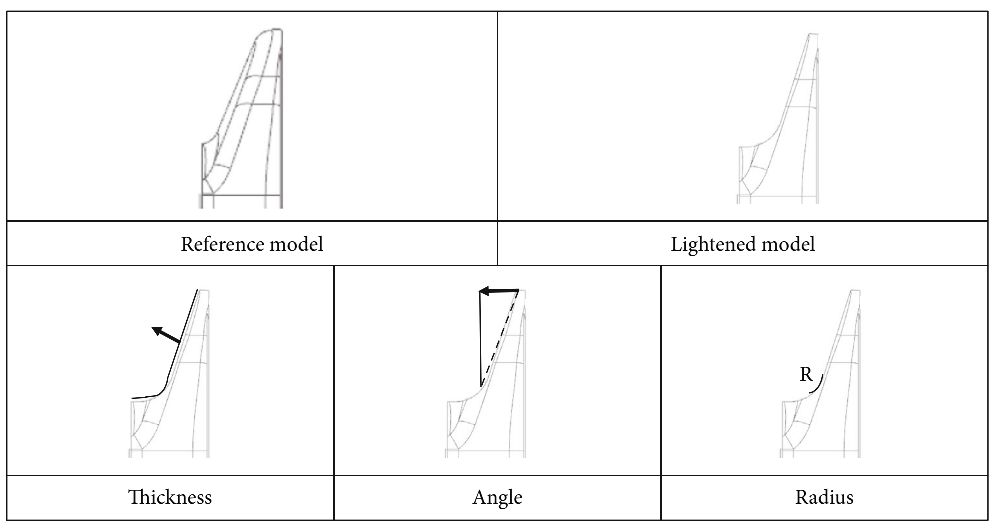

Figure 2: Candidate crank web design sketches.

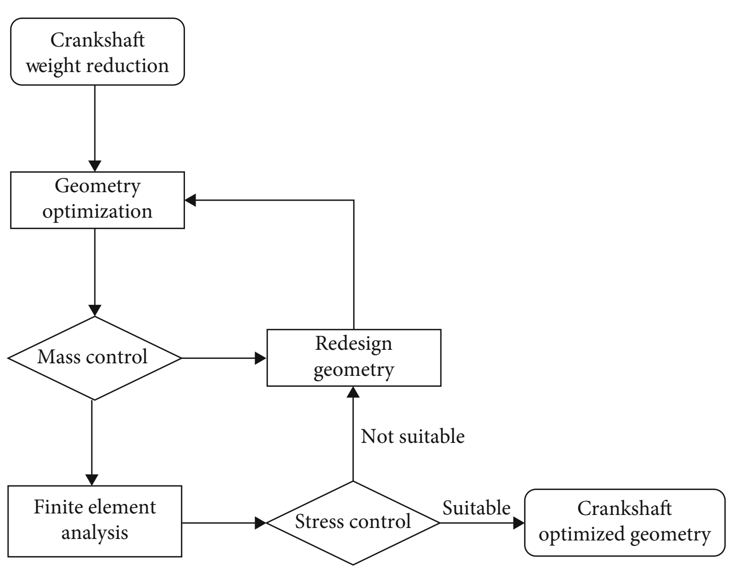

Figure 3: Optimization flow chart.

Table 2: Design iterations.

Iteration	Thickness [mm]	Angle [°]	Radius [mm]	Δ mass [%]
Reference	—	—	—	0
#0 (Manual)	0	0	10	-18.8
#1	1	0	10	-17.9
#2	0	5	10	-16.4
#3	0	0	20	-18.0
#4	0	5	20	-15.6
#5	1	5	10	-15.2
#6	1	0	20	-17.2
#7	1	5	20	-14.1

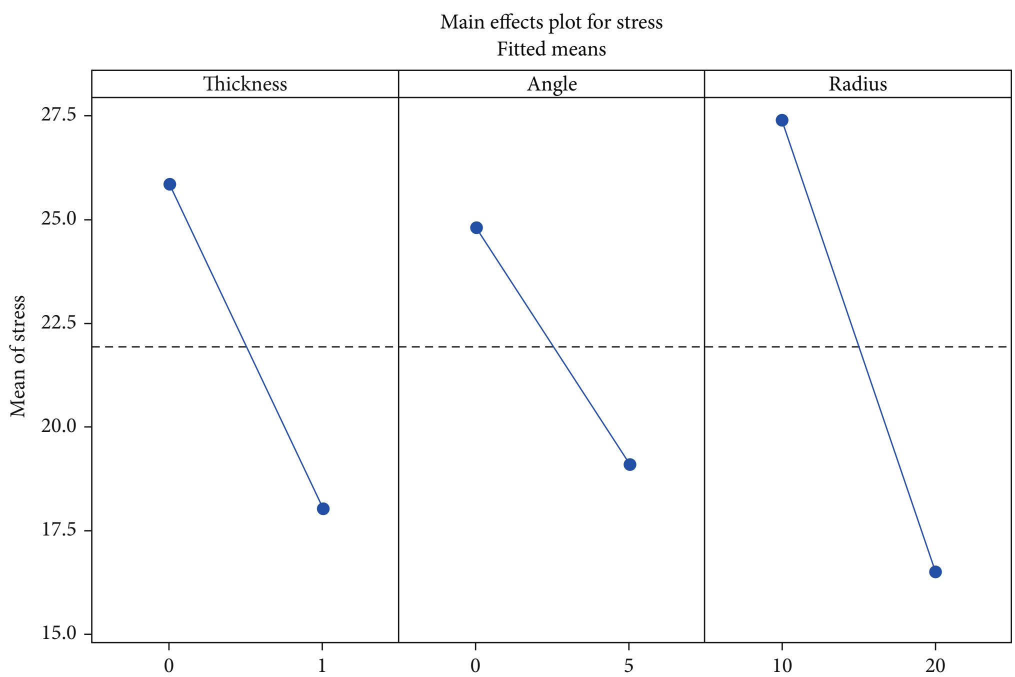

Figure 4: Stress main effects plot.

Table 3: Additional design iterations.

Iteration	Thickness [mm]	Angle [°]	Radius [mm]	Δ mass [%]
Reference	—	—	—	0
#8	0	0	30	-17.6
#9	1	0	30	-16.1
#10	0.5	0	30	-16.8

It was identified that increasing the web angle was the iteration reducing the weight the least and increasing the stress the most, while increasing the radius was the iteration reducing the weight the most and increasing the stress the least, and 3 additional designs were developed as shown in Table 3. In the designs, the web angle and the radius were 0° and 30 mm, respectively, and the web was thickened by 0, 1, and 0.5 mm, respectively. In iteration #10, the increase in stress compared to the reference model was quite close to 15.0%, which led to the lightest geometry. The stress results are provided in Chapter 4.

3.3. Finite Element Analysis. Finite element analysis was utilized to simulate working conditions enables the products to be evaluated virtually before testing a prototype. According to the results, rapid optimization processes can be realized without manufacturing and testing all the iterations [25].

3.3.1. Material. The raw material used to create the designed crankshaft was AISI 4140 [26]. The 4140 steel is a low-alloy material containing chrome, molybdenum, and manganese to improve the parameters of resistance and hardenability [27]. This easy-to-supply material, which is commonly used in the industry, is highly suitable for use in a crankshaft due to its toughness, fatigue strength, and resistance to abrasion and impact. The properties of the AISI 4140 steel used are shown in Table 4.

Table 4: Properties of material.

Property	Unit	Value
Tensile strength	MPa	1100
Yield strength	MPa	900
Young's modulus	MPa	212000
Poisson's ratio	[]	0.28
Density	g/cm^3	7.85
Melting point	$^{\circ}$C	1416
Thermal expansion coefficient (@0-100°C)	μm/m$^{\circ}$C	12.2
Thermal conductivity (@100°C)	W/mK	42.6

3.3.2. Meshing. Using tetrahedral elements to create finite element mesh in complex geometries which are manufactured by casting or forging, such as the crankshaft, provides great convenience. Thus, in the complex geometric regions of the crankshaft, second order tetrahedral elements were used. However, the critical stress regions, the fillets on the main bearings and the crank pins as shown in Figure 5, inherently allow for a more controllable mesh structure with their cylindrical features. These stress-critical areas on the crankshaft should be particularly focused, and the mesh structure should be created with more delicate and smaller elements. For this reason, the second-order hexahedral elements (Solid186) were used in these regions.

In general, as the number of elements decrease, the possibility of deviating from actual stress values increases especially in the regions where the stress gradient is high. In fillet regions, a finite element mesh structure was formed with at least 6 elements for the 90-degree margin. Reading accurate stress values from the elements is also directly related to the closeness of the element shapes to the ideal shape as well as the size of the elements as in the many cases. The closeness of elements to the ideal shape can be checked by utilizing some well-known parameters, such as the aspect ratio and the Jacobian ratio. In addition to these two parameters, the element quality values, which offer general information about the closeness to the ideal shape, were also checked within the scope of this study. All these parameters can be checked rapidly by ANSYS 20R1. The ranges of the relevant parameters for the critical stress regions in this study are determined as in Table 5. The finite element model was developed as fit to these ranges.

The Figure 6 shows the mesh appearance of the main bearing fillet region, which is a critical stress location, with the elements' Jacobian ratio values.

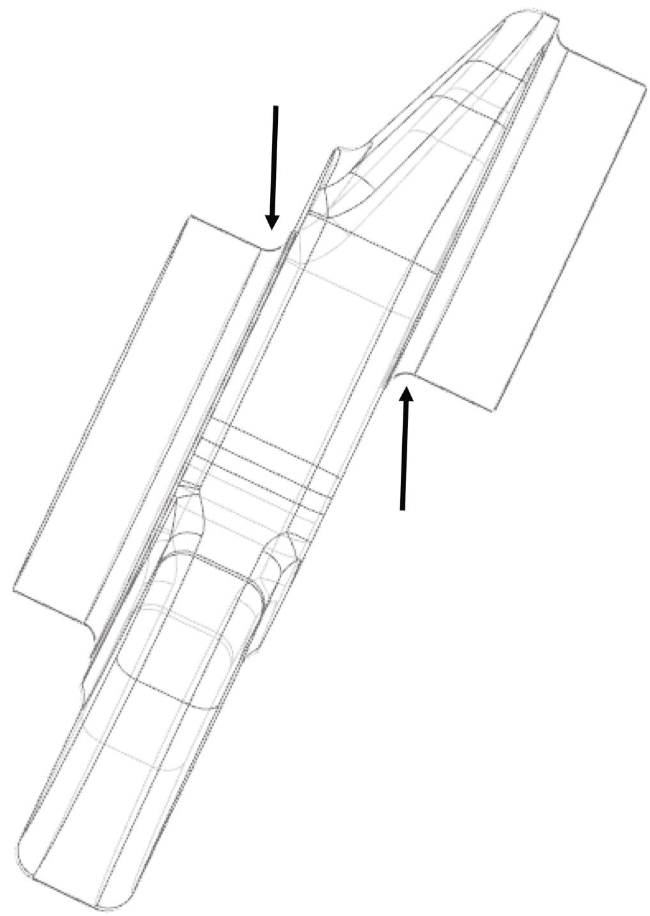

Figure 5: Stress critical zones.

Table 5: Values of control parameters.

Mesh metric	PSE	Min value	Max value
Aspect ratio	1.0	1.0	3.0
Jacobian ratio	1.0	0.7	1.0
Element quality	1.0	0.7	1.0

3.3.3. Boundary Conditions. Dividing the crankshaft and using a small sub-model in finite element analyses, for comparison of any two models, is possible. This method is used to get quick results in simpler analyses. The symmetrical crankshaft is divided into quarters and a quarter slice that simulates the whole is formed. However, defining strict boundary conditions, such as symmetry conditions, could deviate the difference in the stress values between the two models, especially while the actual displacements at the boundary conditions are not provided. This deviation can occur especially when the stiffness difference between the two models is higher. Therefore, the crankshaft was modeled as a whole part and parts such as bearings, caps, and the cylinder block were included in the model with a low mesh density.

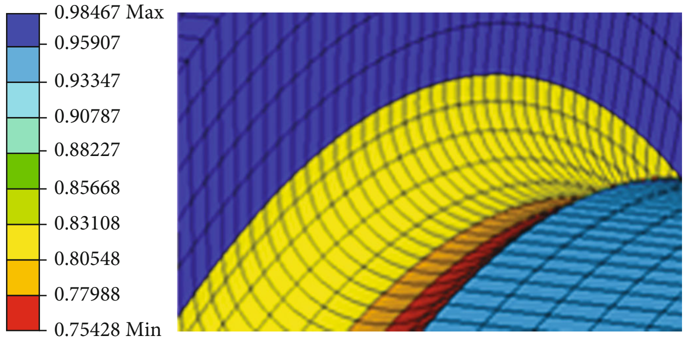

Figure 6: Jacobian ratio values at main journal fillet.

Although torsion can also have an impact on the crankshaft, this study examined the impact of bending on the crankshaft for comparison purposes. Accordingly, the highest stress values in the critical regions, were obtained in two different static analysis load steps. These load steps include the circumstances when the highest forces from the pistons are delivered to the crank pins on the left and right sides, respectively, of the 3rd main bearing. The angular positions of the crankshaft were adjusted to represent these conditions. The load coming from the pistons was obtained from AVL Excite analyses. In ANSYS, it was defined by a sinusoidal distribution on rod journals.

The whole finite element model was fixed tangentially from the upper surface of the cylinder block and vertically from the slot of the main studs of the cylinder block as suitable with the loading conditions. The axial motion of the crankshaft is limited by connecting its web to the cylinder block where the axial thrust bearing locates.

3.3.4. Contact Modeling of Journal-Bearing Interface. The contact algorithms, which also define the contact stiffness, can be directly effective on the deformations especially in the locations close to the contact regions. Therefore, a contact algorithm is supposed to represent the actual contact behavior between the parts especially for the contacts near the stress critical regions. The interface between the main bearing journals and the bearing has a partial gap filled by a layer of oil. The highly non-linear contact stiffness behavior due to the oil film was defined with an exponential function in the pure penalty algorithm in ANSYS. Contacts between other parts were tied by MPC algorithms.

4. Results

A reference model was developed as a part of the study. Weight was reduced manually on the web areas of the reference crankshaft. Three parameters were changed in this model to create 7 candidate designs. The correlation between the input and output parameters of these 7 iterations was calculated by a sensitivity analysis and 3 more designs were developed. Thus, 12 models were analyzed in total. Stress values were calculated using static analyses and an increase of 15.0% was targeted with the highest possible weight reduction. The obtained results are shown in Table 6. Due to the information security, the results are not provided as numerical values but as a percentage change.

Table 6: Analysis results.

Iteration	Δ mass [%]	Δ stress [%]
Reference	0	0
#0 (Manual)	-18.8	+34.2
#1	-17.9	+26.1
#2	-16.4	+28.7
#3	-18.0	+24.2
#4	-15.6	+16.3
#5	-15.2	+20.5
#6	-17.2	+15.7
#7	-14.1	+10.8
#8	-17.6	+17.0
#9	-16.1	+11.9
#10	-16.8	+14.4

With manual reduction, an 18.8% weight decrease, and a 34.2% stress increase were achieved on the reference model. The result showed that among the all iterations, this version was the one with the highest weight reduction increasing the stress the most.

In iterations #1, #2, and #3, in which only single variable was used, increasing the web angle from 0 to 5° was the iteration that reduced the weight the least and increased the stress the most, while increasing the radius from 10 to 20 mm was the iteration that reduced the weight the most and increased the stress the least.

In iterations #4, #5, and #6, where double variables were used, thickening the web by 1 mm and increasing the web angle from 0 to 5° was the iteration that reduced the weight the least and increased the stress the most, while thickening the web by 1 mm and increasing the radius from 10 to 20 mm was the iteration that reduced the weight the most and increased the stress the least.

In iteration #7, where three variables were used, a 14.1% weight decrease, and a 10.8% stress increase were achieved. This result showed that among all iterations, this version

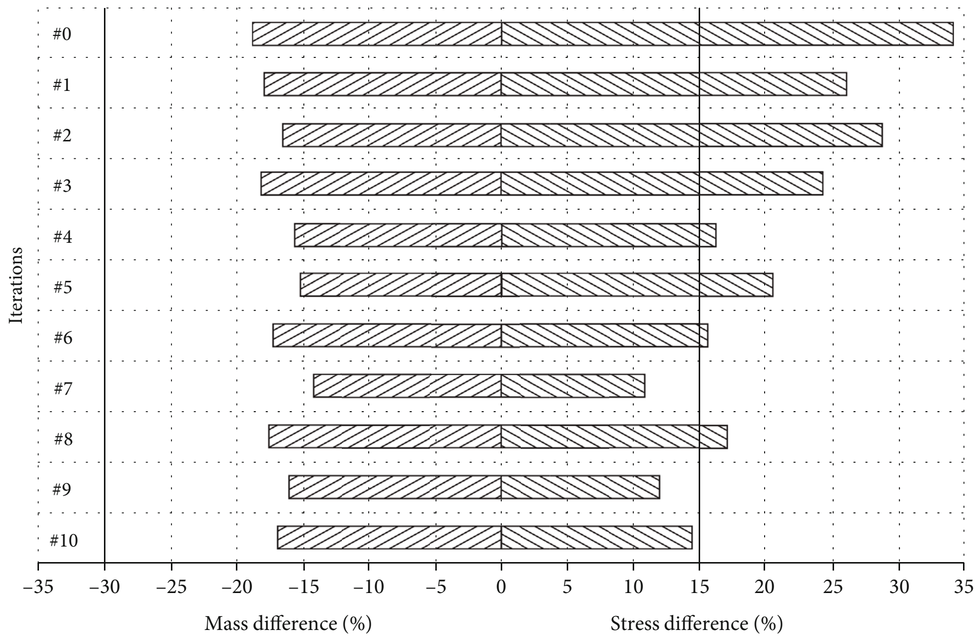

Figure 7: Stress and mass difference of iterations.

had the highest weight reduction and increased the stress the most.

Following the first 7 manually and heuristically developed iterations, it was observed that the weight reduction potential of the crankshaft continued. The correlation between the input and output parameters of the first 7 iterations was calculated by using the sensitivity analysis on Minitab 2019.1.1 and 3 new geometric models were developed corresponding to 3 new sets of input parameters. Among iterations #8, #9, and #10 changes of single or double variables were determined. The iteration reducing the weight the most was the one where the radius was increased from 10 mm to 30 mm. It was observed that the increase in the stress value approached quite close to 15.0% and the lightest possible geometry was achieved compared to the reference model in iteration #10 by thickening the web by 0.5 mm and increasing the radius from 10 mm to 30 mm.

The stress increase values corresponding to weight decrease values obtained in the study are demonstrated in Figure 7.

5. Conclusions

The following studies were carried out on the crankshaft of a 4 cylinder 250 HP compression ignition engine with a volume of 2499 cm^3 designed for use in aircraft:

(i) Following the analysis of the reference model, the target was to achieve the lightest geometry corresponding to a maximum increase of stress by 15.0%.

(ii) The reference crankshaft was modeled by using the Siemens NX software and iteration #0 was developed by performing manual reductions on this model

(iii) A weight reduction by up to 18.8% was observed in model #0 that did not meet the stress limit

(iv) 3 different parameters were identified in iteration #0 by focusing on the web sections of the crankshaft and 7 candidate sets of parameters were developed, each one of them corresponds to different iterations

(v) Results for all iterations were achieved on the ANSYS software by using static stress analyses. Tension stress values were focused on and the maximum principal stress values were read. The minimum increase in stress was 10.8%, which was achieved in iteration #7 where all 3 parameters were applied

(vi) It was observed that the weight reduction potential of the crankshaft was sustained after the first 7 iterations. Therefore, 3 new iterations were developed based on the sensitivity among input and output parameters by analyzing the results of the first 7 iterations using the Minitab software

(vii) In the final case, it was observed that the lightest geometry was achieved with a 14.4% stress increase by thickening the web by 0.5 mm and increasing the radius from 10 mm to 30 mm and it was decided to make use of the relevant iteration in manufacturing processes

(viii) A similar iteration process can be performed using algorithms such as response surface in finite element software. However, in this study, thanks to experience, the number of iterations was decreased and a heuristic, but the rapid approach was adopted

(ix) The next study is being planned as an optimization study to focus on the change of lifetime of the parts by comparing their fatigue strengths

Nomenclature

AISI: American Iron and Steel Institute
CAD: Computer Aided Design
cm^3: Cubic Centimeter
DOE: Design of Experiments
EBW: Electron Beam Welding
HP: Horse Power
kW: Kilowatt
mm: Millimeter
MPa: Megapascal
MPC: Model Predictive Control
NVH: Noise, Vibration and Harshness
PSE: Perfectly Shaped Element
rpm: Revolutions per Minute
3D: Three Dimensional
#: Number.

Data Availability

Authors make data available on request. In this case, who should be contacted with the corresponding author Serkan Galata for the data. E-mail address: serkan.galata@gmail.com

Conflicts of Interest

The authors declare that they have no conflicts of interest.

Acknowledgments

This technical paper was supported by TEI – TUSAŞ Engine Industries Inc. (Eskisehir, Turkey) with the project number 2020-PMM-3885-01 and was created within the scope of the corresponding author's PhD thesis.

References

[1] S. Galata, *Experimental Investigation of Water Injection on the Performance and Exhaust Emissions of an Internal Combustion Engine, [M.S. thesis]*, Yildiz Technical University, Graduate School of Science and Engineering, Mechanical Engineering Department, Istanbul, Turkey, 2017.

[2] J. B. Heywood, *Internal Combustion Engine Fundamentals*, McGraw-Hill, Inc., New York, USA, 1988.

[3] K. D. Prasad, K. V. J. P. Narayana, and N. Kiranmayee, "Design and stress analysis of crankshaft for single cylinder 4 stroke diesel engine," *International Journal of Engineering Research & Technology*, vol. 7, no. 11, pp. 154–159, 2018.

[4] A. Garro and V. Vullo, "Some consideration on the evaluation of thermal stresses in combustion engine," *SAE Transactions*, vol. 87, pp. 2563–2592, 1978.

[5] S. Baragetti, "Design criteria for high power engines crankshafts," *The Open Mechanical Engineering Journal*, vol. 9, no. 1, pp. 271–281, 2015.

[6] O. Keita, T. Hedhli, and J. Bessrour, "Model for dynamic behavior of the crankshaft of an air cooled diesel engine subjected to severe functioning," *International Journal of Automotive Technology*, vol. 15, no. 5, pp. 823–833, 2014.

[7] M. Kumar and S. N. Prajapati, "Crankshaft design optimally and failure analysis: a review," *International Journal of Science and Research*, vol. 6, no. 7, pp. 425–430, 2017.

[8] F. Liu, C. Sun, Y. Li, and Y. Shang, "Performance analysis and optimization design of exhaust system for turbocharging diesel engines," *International Journal of Automotive Technology*, vol. 22, no. 3, pp. 735–745, 2021.

[9] G. Mathan, J. Daniel, P. Vishnu, and V. Satyanarayana, "Impact of web and counterweight shape factors on crank shaft design for better strength and optimised geometry," *IOP Conference Series: Materials Science and Engineering*, vol. 1128, article 012045, 2021.

[10] M. Sangeetha, P. Boomadevi, A. S. Khalifa, K. Brindhadevi, and M. Sekar, "Vibration, acoustic and emission characteristics of the _chlorella vulgaris_ microalgae oil in compression ignition engine to mitigate environmental pollution," *Chemosphere*, vol. 293, article 133475, 2022.

[11] S. Ge, A. Pugazhendhi, M. Sekar et al., "PM emissions - assessment of combustion energy transfer with *Schizochytrium* sp. algal biodiesel and blends in IC engine," *Algal biodiesel and blends in IC engine, Science of Total Environment*, vol. 802, article 149750, 2022.

[12] A. P. Druschitz, D. C. Fitzgerald, and I. Hoegfeldt, "Lightweight crankshafts," in *SAE – American Society of Automotive Engineers Technical Paper Series*, United States, 2006.

[13] FEV Europe GmbH, "Cranktrain design optimized for reducing weight and friction supported by coupled CAE tools," 2020, https://www.fev.com/fileadmin/user_upload/Media/TechnicalPublications/Design/OptimizedCranktrainDesignSupportedbyCAE.pdf.

[14] P. Horvath and J. Egert, "Stress analysis and weight reduction of a one-cylinder engine crankshaft," *Acta Technica Jaurinensis*, vol. 8, no. 3, pp. 201–217, 2015.

[15] M. Zoroufi and A. Fatemi, "A literature review on durability evaluation of crankshafts including comparisons of competing manufacturing processes and cost analysis," in *26th Forging Industry Technical Conference*, Chicago, USA, 2005.

[16] V. Angelopoulos, *A Model-Based Design Approach to Redesign a Crankshaft for Powder Metal Manufacturing, KTH Industrial Engineering and Management Machine Design, [M.S. thesis]*, KTH - Royal Institute of Technology, Stockholm, Sweden, 2015.

[17] L. A. Archer, *Development of High-Performance Cast Steel Crankshafts, [M.S. thesis]*, The University of Iowa, Graduate College, Mechanical Engineering Department, Iowa, USA, 2016.

[18] J. R. Williams and A. Fatemi, *Fatigue performance comparison and life predictions of forged steel and ductile cast iron crankshafts*, Forging Industry Educational Research Foundation and American Iron and Steel Institute Final Project Report, Toledo, USA, 2007.

[19] M. Hingne, R. Dwivedi, R. V. Choudri, and S. Chalotre, "Analysing the effect of weight reduction of crankshaft on the pressure parameter inside cylinder of single cylinder SI engine," *Materials Today: Proceedings*, vol. 47, pp. 6296–6300, 2021.

[20] M. C. Cevik, M. Rebbert, and F. Maassen, "Weight and friction optimized cranktrain design supported by coupled CAE tools," in *SAE – American Society of Automotive Engineers Technical Paper Series*, United States, 2009.

[21] I. Papadimitriou and K. Track, "Lightweight Potential of Crankshafts with Hollow Design," *MTZ Worldwide*, vol. 79, no. 1, pp. 42–45, 2018.

[22] Honda Racing Formula One, K. Mizoue, Y. Kawahito, and K. Mizogawa, "Development of hollow crankshaft," 2021, http://www.f1-forecast.com/pdf/F1-Files/Honda/F1-SP2_31e.pdf.

[23] P. Thejasree, G. D. Kumar, and S. L. Prasanna Lakshmi, "Modelling and analysis of crankshaft for passenger car using ANSYS," *Materials Today: Proceedings*, vol. 4, no. 10, pp. 11292–11299, 2017.

[24] L. Piancastelli and S. Cassani, "On the conversion of automotive engines for general aviation," *ARPN Journal of Engineering and Applied Sciences*, vol. 12, no. 13, pp. 4196–4203, 2017.

[25] Y. Okur, *Maximization of Natural Frequencies of an Engine Bracket with Bidirectional Evolutionary Topology Optimization Method, [M.S. thesis]*, Istanbul Technical University, Graduate School, Aeronautics and Astronautics, Istanbul, Turkey, 2019.

[26] B. Stojanovic and J. Glisovic, "Automotive Engine Materials," in *Reference Module in Materials Science and Materials Engineering*, University of Kragujevac, Kragujevac, Serbia, 2016.

[27] SAE – American Society of Automotive Engineers Aerospace Material Certification, *AMS6382 Revision R, Aerospace Material Certification AMS6382 Steel, Bars, Forging, and Rings – SAE 4140*, 2018.